Original brief communication

Neuroligin fragments as blood-based biomarkers for early detection of Alzheimer's disease.

Milton Guilherme Forestieri Fernandes[1], Maxime Pinard[2], Esen Sokullu[2], Jean-François Gagnon[3,4], Frédéric Calon[5,6], Benoit Coulombe[2], the Consortium for the early identification of Alzheimer's disease-Quebec (CIMA-Q)*, Jonathan Brouillette[1,]**

Affiliations :

1 Department of Pharmacology and Physiology, Université de Montréal, Montreal, QC, Canada, H3T 1J4.

2 Translational Proteomics Laboratory, Institut de Recherches Cliniques de Montréal, Montreal, QC, Canada, H2W 1R7.

3 Department of Psychology, Université du Québec à Montréal, Montreal, QC, Canada, H2X 3P2.

4 Centre for Advanced Research in Sleep Medicine, Hôpital du Sacré-Coeur de Montréal, Centre intégré universitaire de santé et de services sociaux du Nord de l'Île-de-Montréal, Montreal, Canada, H4J 1C5.

5 Faculty of Pharmacy, Laval University, Quebec, QC, Canada, G1V 0A6.

6 Neuroscience Axis CHU de Québec Research Center – Laval University, Quebec, QC, Canada, G1V 4G2.

* The data used in the preparation of this article were obtained thanks to the Consortium for the early identification of Alzheimer's disease – Quebec (CIMA-Q; cima-q.ca). A list of researchers involved in the design of CIMA-Q can be found on the cima-q.ca website. These researchers contributed to the establishment of protocols, the implementation of the research infrastructure, the recruitment and follow-up of participants, the obtaining of data, the maintenance of biological and ex-vivo samples, and certain derived data.

**** Corresponding authors:**

Jonathan Brouillette, jonathan.brouillette@umontreal.ca

ABSTRACT

Biomarkers for early detection of Alzheimer's disease (AD) are essential for improving treatments. Fragments of the synaptic protein neuroligins (NLGNs) are released into the blood due to synaptic degeneration, which occurs in the early stages of AD. Using MS2-targeted mass spectrometry, we assessed the potential of NLGN fragments as blood-based biomarkers for amnestic mild cognitive impairment (aMCI), a prodromal stage of AD. We found higher blood levels of certain NLGN fragments in both aMCI and AD patients compared to healthy subjects and elderly with subjective cognitive disorder (SCD) from the CIMA-Q cohort. Within these same samples, the levels of Tau phosphorylated at various epitopes (pTau181, pTau217, and pTau231) were higher in AD subjects but not in aMCI individuals. Our results suggest that synaptic proteins such as NLGNs could serve as effective biomarkers for detecting the disease in its prodromal stage. This early detection could accelerate diagnosis, prevention, and therapeutic intervention before neurodegeneration leads to irreversible brain damage.

MAIN

Currently, there is no treatment to prevent or cure Alzheimer's disease (AD), the most common cause of dementia in the elderly. Identifying such a treatment requires the early detection of the disease, allowing for therapeutic interventions while individuals remain autonomous, active, and maintain a good quality of life. It is well-established that AD dementia is preceded by two transitional stages: subjective cognitive disorder (SCD), followed by amnestic mild cognitive impairment (aMCI)[1,2]. However, there is still an urgent need for reliable biomarkers for these stages.

Synapse loss is observed in prodromal AD and correlates with cognitive decline of the patients[3-5]. Although it is hypothesized that synaptic loss is generally induced by neuronal hyperactivity rather than hypoactivity[6-8], little is known about the synaptic proteins affected by hyperactivity of glutamatergic transmission in AD. Neuroligin-1 (NLGN1) is a post-synaptic transmembrane protein exclusively localized on glutamatergic synapses and is important for synapse formation, maintenance, and plasticity[9,10]. Previous work has demonstrated that neuronal hyperactivity promotes the cleavage of NLGN1 extracellular domain[11,12], which is then released into the blood [13,14].

Recently, our laboratory found that individuals with aMCI have lower levels of NLGN1 in the hippocampal brain region[15]. Also, the level of NLGN1 was found to be decreased even more in AD patients compared to aMCI and age-matched, non-demented control (CTL) subjects[15], suggesting that measuring the level of NLGN1 could help discriminating aMCI individuals from AD patients or healthy elderly and therefore follow disease progression.

There is evidence for synaptosomal degeneration in GABAergic inhibitory interneurons in some brain regions of AD patients and animal models[16-19]. Given that the neuroligin isoform NLGN2 is found solely at inhibitory synapses, we also sought to evaluate if this other neuroligin species is altered in the plasma of aMCI and early AD subjects. Interestingly, it was found recently that levels of both NLGN1 and NLGN2 are increased in the cerebrospinal fluid (CSF) of preclinical AD patients using targeted mass spectrometry[20].

Thus, we hypothesized that neuronal hyperactivity observed in prodromal AD leads to the cleavage of neuroligins (NLGNs), which progressively increases the concentration of soluble NLGN fragments in the plasma of aMCI and AD subjects compared to CTL elderly. Given that blood-based biomarker assays are simple, minimally invasive and cost-effective, measuring plasma level of NLGN fragments could have a direct impact on the development of therapeutics.

To test our hypothesis, we developed an ultra-sensitive technique for quantifying blood levels of NLGN1 and NLGN2. This technique involves Protein Affinity Capture coupled with quantitative Mass Spectrometry (PAC-qMS) to analyze NLGN1 and NLGN2 together in plasma samples from the Consortium for the early identification of Alzheimer's Disease - Quebec (CIMA-Q) cohort. The demographic characteristics of this cohort are detailed in Extended Data Table 1. We compared the plasma concentrations of NLGN fragments and their potential as biomarkers for aMCI and early AD with those of phosphorylated Tau (pTau) at various epitopes (pTau181, pTau217, and pTau231), which have been identified as promising early biomarkers of AD[21]. The clinical evaluation, inclusion and exclusion criteria, blood sample processing, and method to analyse tau levels for CIMA-Q participants have been previously described in detail[22].

A total of 107 samples from the CIMA-Q dataset were evaluated. Of these, 101 were successfully quantified. The breakdown of these samples by diagnosis is shown in Fig. 1a. Fig. 1b displays the quantities of samples in which the five fragments of NLGN2 and the single fragment of NLGN1 were quantified. NLGNs were quantified by using standard curves produced with known amounts of each NLGN (Extended Data Fig. 1). The sequence of amino acids of these fragments are in Extended Data Table 3, and their positions in both proteins are shown in Extended Data Fig. 2. NLGN2 fragments 1 and 2 and the NLGN1 fragment were identified in most of the samples, while other fragments were present in fewer samples (Fig. 1b). The influence of risk factors for AD such as the presence of APOE4 genes, sex, age and years of education on the level of NLGN fragments was evaluated (Extended Data Fig. 3). Only the presence of two alleles of APOE4 was associated with a higher level of NLGN2 fragment 1 (Extended Data Fig. 3a).

The level of NLGN2 fragment 1 was significantly higher in subjects with aMCI compared to CTL and those with SCD (Fig. 1c), even after considering the correction for the APOE4 influence. The average level of NLGN2 fragment 5 showed a tendency to be higher in aMCI compared to CTL (p-value of 0.078; Fig. 1g). The level of NLGN1 fragment was significantly higher in AD patients compared to individuals with SCD (Fig. 1h). Additionally, we observed that pTau181, pTau217, and pTau231 were highly effective in differentiating AD patients from CTL, SCD, or aMCI subjects (Fig. 1i, j, k). However, none of these pTau biomarkers could distinguish aMCI from CTL or SCD participants, at least in the samples used here to determine blood levels of NLGN1/2. When analyzing a larger number of samples from the CIMA-Q cohort, a significant difference was observed between SCD and aMCI subjects (data not shown). Some past studies have also shown the efficiency of plasma pTau as a biomarker for distinguishing clinical AD and for detecting aMCI, though with a lower degree of accuracy[23-25]. Because NLGN1/2 fragments can distinguish between different stages of the disease (CTL *vs* aMCI, SCD *vs* aMCI, and SCD *vs* AD), they could be useful for monitoring the progression of the illness.

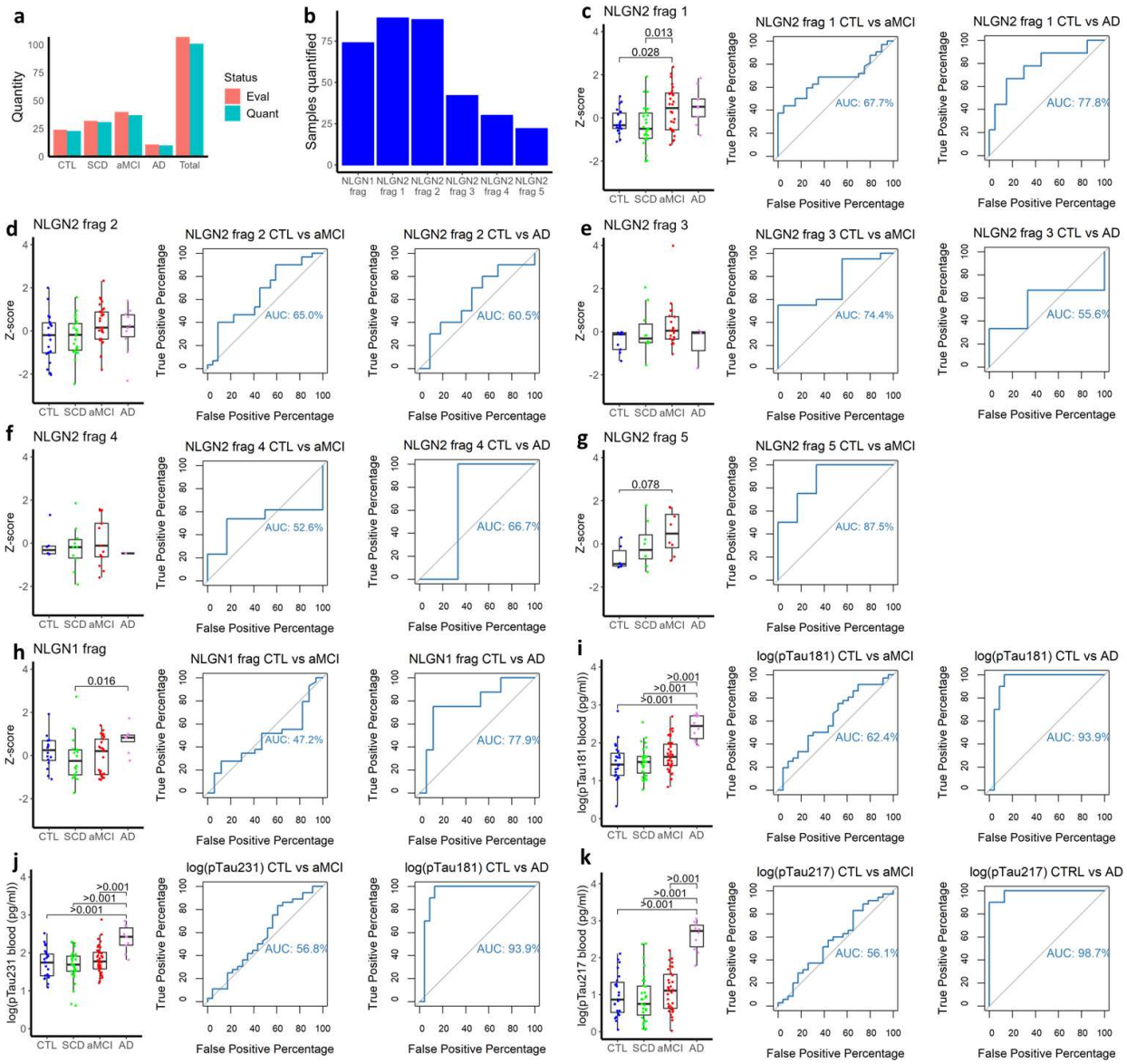

Fig. 1: Blood concentration of NLGN2 fragments indicates amnestic mild cognitive impairment (aMCI) diagnosis more precisely than blood concentration of phosphorylated Tau fragments. **a,** Quantity of samples evaluated and quantified by diagnostic group. **b,** Number of samples in which each peptide was quantified. **c-h,** NLGN fragments levels in blood by diagnostic group, and respective receiver operating characteristic (ROC) curves with area under the curve (AUC) for aMCI and AD in relation to CTL. Z-score corresponds to the normalized value corrected for batch effect **i-k**, Phosphorylated Tau fragments levels in blood by diagnostic group, and respective ROC curves with AUC for aMCI and AD in relation to CTL. Significant levels correspond to the p-value calculated by Tukey test. CTL: control, SCD: subjective cognitive disorder, aMCI: amnestic mild cognitive impairment, AD: Alzheimer's disease.

To further evaluate the potential of NLGN and pTau as biomarkers, we analyzed receiver operating characteristic (ROC) curves and calculated the area under the curve (AUC) for all fragments

comparing aMCI and AD patients against the control group (Fig. 1c-k). For aMCI, NLGN2 fragments 1, 2, 3 and 5 have higher AUC than all pTau (Fig, 1c, d, e, g, i, j, k). In contrast, when comparing AD to CTL, pTau presented higher AUC values (Fig. 1 i, j, k). We have also observed a significant correlation between the blood level of the NLGN1 fragment, the NLGN2 fragment 1, and all three pTau (Fig. 2), indicating that these biomarkers can be used in tandem to better predict AD progression. The correlation between the other NLGN2 fragments and each pTau was not significant (Extended Data Fig.4).

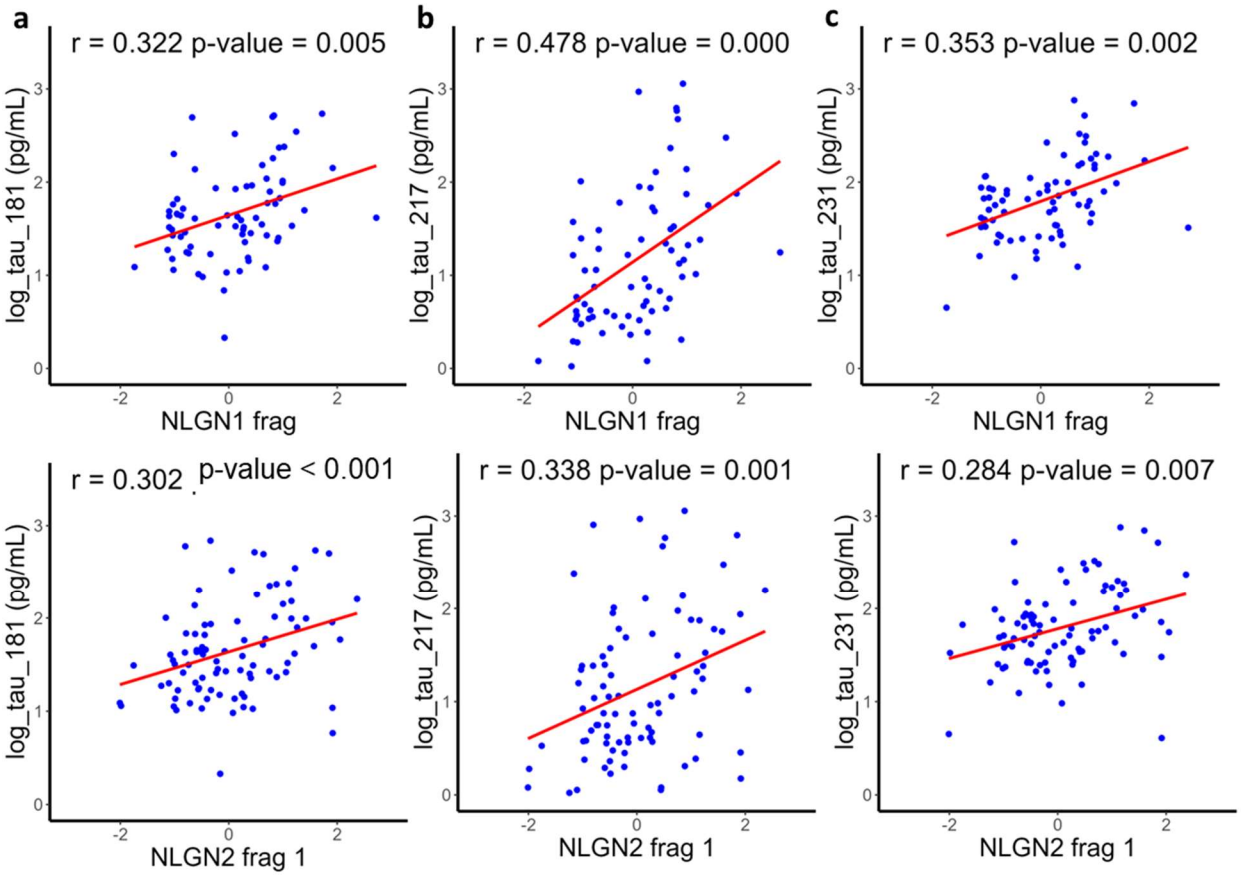

Fig. 2: Blood concentration of some NLGN fragments correlates with blood concentration of phosphorylated Tau.a-c, Correlation between blood concentration of selected fragments of NLGN1 and NLGN2, and blood concentration of phosphorylated Tau. The Pearson correlation coefficient and significant levels are indicated at the top of each plot. The levels of NLGN fragments correspond to the normalized value corrected for batch effect.

To determine if changes in plasma levels of NLGNs are specific for prodromal AD, we used blood samples of individuals in the prodromal stages of neurodegenerative synucleinopathies, including Parkinson's disease (PD) and dementia with Lewy bodies (DLB). Since the large majority of individuals with REM behaviour disorder (RBD) developed synucleinopathies[26], this condition can be used as a marker of prodromal synucleinopathies. The demographic characteristics of the

cohort we used can be consulted in the Extended Data Table 2. We observed no significant difference between RBD patients who developed DLB or PD compared to controls or non-converter (NC) individuals with RBD (Extended Data Fig. 5). In most cases, NLGN1 and NLGN2 fragments were under the limit of quantification or not even detected in these participants, suggesting that NLGNs might be a specific marker of prodromal stages of AD.

In conclusion, since synapse dysfunction and loss precede neuronal death, identifying changes in synaptic proteins in the blood of individuals with aMCI and early AD would be highly valuable for earlier disease detection and the development of therapeutics before neurodegeneration causes significant cognitive impairments. In this study, we found that blood levels of certain NLGN1/2 fragments are increased in the prodromal stage of AD. These fragments allow differentiation between various stages of the disease and correlate with pTau181, pTau217, and pTau231. Overall, these results suggest that NLGN fragments could potentially serve as a primary care screening test and be incorporated into a panel of early biomarkers to more accurately track disease progression in clinical practice and trials.

METHODS

CIMA-Q cohort

The data used in this manuscript were partially obtained from the Consortium for the early identification of Alzheimer's disease – Quebec (CIMA-Q), established in 2013 with initial funding from FRQS-Pfizer. The primary objective of CIMA-Q was to establish a cohort of clinically, cognitively, and neuroimaging-characterized elderly men and women, and to collect blood samples with the following goals: (1) to establish an early diagnosis of Alzheimer's disease; (2) to make a well-characterized cohort available to the scientific community; (3) to identify new therapeutic targets to prevent or slow cognitive decline and Alzheimer's disease; and (4) through subsequent clinical studies. Further details on recruitment methods, exclusion and inclusion criteria, testing materials, and general methodology for the CIMA-Q project can be found in Belleville et *al*.[22]. Diagnostic criteria for AD and aMCI were based on the National Institute on Aging–Alzheimer's Association and were described in detail in Belleville et *al*.[22].

PAC-qMS sample preparation

5 µg of specific antibody against both NLGN1 (Bio-techne, AF4340) and NLGN2 (Bio-techne, AF5645) was coupled overnight at 37°C to 1 mg of dynabead epoxy M-270 (Thermofisher scientific, Cat #: 14311D) and equilibrated according to the manufacturer's specifications. Samples and calibration points were prepared by using similar amounts of either patient plasma or commercially availed pooled plasma (Innovative research, Cat #: IPLANAC50ML), respectively. Each sample was diluted in a final volume of 250 µL with 1x PBS (Wisent, Cat #: 311-010-EL). Calibration curves were generated by spiking diluted pooled plasma with known amounts of the recombinant NLGN1 protein (Cedarlane, Cat #: TP307524) and NLGN2 protein (Bio-techne, Cat #: 5645-NL_050) (0, 1, 2, 5, 10, 25, 100 ng). A calibration curve was prepared for each set of 34 tested patient plasma. Equilibrated antibody-coupled magnetic bead was added to the plasma samples (patient or calibration curve points) and NLGN1-NLGN2 capture was performed at 4°C for 1 h on a rotator shaker. Magnetic beads were washed 6 times with fresh HBSEP buffer (10 mM

Tris-HCl pH 8.0, 150 mM NaCl, 3 mM EDTA, 0.005% Tween20) and 4 times with water. Captured proteins were eluted with an 33% acetonitrile and 0.4% trifluoroacetic acid elution buffer, dried down by using a speed vacuum centrifuge (Eppendorf) and stored at -70°C until sample digestion. The dried pellets were resuspended in 20 µL of 6 M urea and 100 mM ammonium bicarbonate. 5 µL of reduction buffer (45 mM dithiothreitol, 100 mM ammonium bicarbonate) was added to each sample and incubated at 37°C for 30 min on a thermomixer (Thermofisher scientific) set at 350 RPM. 5 µL of alkylation buffer was added to each tube (100 mM iodoacetamide, 100 mM ammonium bicarbonate) and peptide alkylation was performed at 24°C for 20 min in the dark. Prior to trypsin digestion, 50 µL of 50 mM ammonium bicarbonate was added to reduce the urea concentration under 2 M. Trypsin solution, 5 µL of 100 ng/µL of trypsin sequencing grade from Promega (Promega, Cat #: V5111), 50 mM ammonium bicarbonate was added to each sample. Protein digestion was performed at 37ºC for 18 h. The protein digests were acidified with 9.4 µL formic acid 5% in water and dried with a speed vacuum centrifuge. Prior to LC-MS/MS, protein digests were re-solubilized under agitation for 15 min in 12 µL of 2% ACN-1% formic acid and spiked with heavy-labeled standard peptides specific to NLGN1 and NLGN2 protein forms (JPT Peptide technologies Gmbh, Volmerstrasse, Germany). These peptides were added for signal normalization and retention time confirmation of one NLGN1 peptide (GNYGLLDLIQAL-R*) and one NLGN2 peptide (FPVVNTAYG-R*) where R* is Arg U-^{13}C6 and U-^{15}N4. Desalting and cleanup of the digests were performed using C18 ZipTip pipette tips (Millipore, Billerica, MA). Eluates were dried down in speed vacuum centrifuge and stored at -20ºC until LC-MS/MS analysis.

Mass spectrometry

Samples were reconstituted under agitation for 15 min in 11 µL of 2% ACN-1% FA and loaded into a 75 µm i.d. × 150 mm Self-Pack C18 column installed in the Easy-nLC II system (Proxeon Biosystems). The buffers used for chromatography were 0.2% formic acid (buffer A) and ACN/0.2% formic acid (buffer B). Peptides were eluted with a two-slope gradient at a flowrate of 250 nL/min. Solvent B first increased from 2 to 35% for 40 min and then from 35 to 85% B for 5 min. The HPLC system was coupled to an Orbitrap Fusion mass spectrometer (Thermo Scientific) through a Nanospray Flex Ion Source. Nanospray and S-lens voltages were set to 1.3-1.8 kV and 60 V, respectively. The capillary temperature was set to 250°C. Targeted MS^2 spectra were acquired in the Orbitrap with a resolution of 30,000, a target value at 5e4 and a maximum injection time of 150 ms. The peptide fragmentation was performed in the HCD cell at a normalized collision energy of 29%. The peptide m/z and retention time used to detect each peptide are listed in the Extended Table 3.

Data analysis

Raw mass spectrometry data was imported in PinPoint (ThermoFisher scientific, Version 1.4.0). Peptide abundance in the calibration curve and each patient sample were calculated using the sum of the area of four transitions per peptides and normalized against the sum of the area of four transition of the heavy-labeled NLGN1 peptide (see Extended Table 3). Injected amount (in ng) was used to determine the standard curve linearity for each peptide and to calculate the linear regression equation (see Extended Data Fig 1b). NLGNs amount (in ng) for each sample was

evaluated by using the regression equation and the concentration in each sample was than calculated. Lower limit of detection (LLOD) and lower limit of quantification (LLOQ) were set as the 3 and 10 times the background level measured in the lowest amount of the calibration curve.

Statistical analysis

All statistical analyses were executed in R.

Normalization and batch effect correction

First, the logarithm to the base two of the blood concentration of the NLGN fragments of all samples was calculated. Then, the mean and the standard variation of these values for each batch in which they were measured was calculated. To normalize the measurements and eliminate the batch effect, the Z-score for each sample was calculated using the following equation:

$$Z_{i,j} = \frac{(C_{i,j} - X_j)}{\sigma_j}$$

Where:

$Z_{i,j}$ = Z-score of the sample i of the batch j

$C_{i,j}$ = Log_2 of the blood concentration of the sample i of the batch j

X_j = Mean of the log_2 of the blood concentration of the batch j

σ_j = Standard deviation of the log_2 of the blood concentration of the batch j

Statistical significance tests

The Shapiro-Wilk test was executed to verify the normality of the measurement, and the Levene's test was used to check homoscedasticity. ANOVA, or the Kruskal-Wallis test in the cases where normality or homoscedasticity were not verified, were performed to assess the differences in the z-score of blood concentration of NLGN fragments, and the log_{10} of blood concentration of the phosphorylated Tau classified by diagnostic. The number of APOE4 alleles and age of participants were assessed as potential co-factors. The Tukey's test was used to evaluate differences between pairs of diagnostic categories. The same analysis was executed between the z-score of blood concentration of NLGN fragments and the number of APOE4 alleles. A t-test was used to compare the differences in the z-score of blood concentration of NLGN fragments between sex of participants.

Correlation analysis

For the assessment of the correlation between the z-score of blood concentration of NLGN fragments and the age and years of education of the participants, as well as the correlation between the z-score of blood concentration of NLGN fragments and the log_{10} of blood concentration of the

phosphorylated Tau, the Pearson correlation coefficient along with chi-square test to evaluate the statistical significance of correlation were calculated.

Receiver operating characteristic (ROC) curves and area under the curve (AUC)

Receiver operating characteristic curves were analyzed with the help of the roc() function of the pROC package in R. First, samples for the two categories to be compared (either CTL *vs* aMCI or CTL *vs* AD) were fitted to a logistic regression model using the glm() function. The fitted values were used as the threshold to determine the number of false positives and true positives at each point of the ROC curve. The area under the curve corresponds to the percentage of the total plot area that is under the ROC curve (set argument print.auc = TRUE when using the roc() function to obtain the AUC value).

Acknowledgement

We are grateful to Denis Faubert, Josée Champagne, Sylvain Tessier, and Marguerite Boulos for their assistance in sample processing and mass spectrometric data acquisition. Thank you to Ronald B. Postuma and Nadia Gosselin for providing samples from the Canadian Biobank for Sleep Research. The CIMA-Q is supported by the Fonds de recherche du Québec – Santé (FRQS) grant, Fonds de recherche du Québec (FRQ) cohort funds, Quebec Network for Research on Aging (RQRV), the Fondation Famille Lemaire, and the Fondation Courtois.

References

1 Anderson, N. D. State of the science on mild cognitive impairment (MCI). *CNS Spectr* **24**, 78-87 (2019). https://doi.org:10.1017/s1092852918001347

2 Vos, S. J. *et al.* Prediction of Alzheimer disease in subjects with amnestic and nonamnestic MCI. *Neurology* **80**, 1124-1132 (2013). https://doi.org:10.1212/WNL.0b013e318288690c

3 Terry, R. D. *et al.* Physical basis of cognitive alterations in Alzheimer's disease: synapse loss is the major correlate of cognitive impairment. *Ann Neurol* **30**, 572-580 (1991). https://doi.org:10.1002/ana.410300410

4 Selkoe, D. J. Alzheimer's disease is a synaptic failure. *Science* **298**, 789-791 (2002). https://doi.org:10.1126/science.1074069

5 Coleman, P. D. & Yao, P. J. Synaptic slaughter in Alzheimer's disease. *Neurobiol Aging* **24**, 1023-1027 (2003). https://doi.org:10.1016/j.neurobiolaging.2003.09.001

6 Busche, M. A. *et al.* Critical role of soluble amyloid-β for early hippocampal hyperactivity in a mouse model of Alzheimer's disease. *Proc Natl Acad Sci U S A* **109**, 8740-8745 (2012). https://doi.org:10.1073/pnas.1206171109

7 Busche, M. A. *et al.* Decreased amyloid-β and increased neuronal hyperactivity by immunotherapy in Alzheimer's models. *Nat Neurosci* **18**, 1725-1727 (2015). https://doi.org:10.1038/nn.4163

8 Targa Dias Anastacio, H., Matosin, N. & Ooi, L. Neuronal hyperexcitability in Alzheimer's disease: what are the drivers behind this aberrant phenotype? *Translational Psychiatry* **12**, 257 (2022). https://doi.org:10.1038/s41398-022-02024-7

9 Südhof, T. C. Neuroligins and neurexins link synaptic function to cognitive disease. *Nature* **455**, 903-911 (2008). https://doi.org:10.1038/nature07456

10 Craig, A. M. & Kang, Y. Neurexin-neuroligin signaling in synapse development. *Curr Opin Neurobiol* **17**, 43-52 (2007). https://doi.org:10.1016/j.conb.2007.01.011

11 Suzuki, K. *et al.* Activity-Dependent Proteolytic Cleavage of Neuroligin-1. *Neuron* **76**, 410-422 (2012). https://doi.org:https://doi.org/10.1016/j.neuron.2012.10.003

12 Peixoto, R. T. *et al.* Transsynaptic signaling by activity-dependent cleavage of neuroligin-1. *Neuron* **76**, 396-409 (2012). https://doi.org:10.1016/j.neuron.2012.07.006

13 Keshishian, H. *et al.* Multiplexed, Quantitative Workflow for Sensitive Biomarker Discovery in Plasma Yields Novel Candidates for Early Myocardial Injury. *Mol Cell Proteomics* **14**, 2375-2393 (2015). https://doi.org:10.1074/mcp.M114.046813

14 Keshishian, H. *et al.* Quantitative, multiplexed workflow for deep analysis of human blood plasma and biomarker discovery by mass spectrometry. *Nat Protoc* **12**, 1683-1701 (2017). https://doi.org:10.1038/nprot.2017.054

15 Dufort-Gervais, J. *et al.* Neuroligin-1 is altered in the hippocampus of Alzheimer's disease patients and mouse models, and modulates the toxicity of amyloid-beta oligomers. *Scientific Reports* **10**, 6956 (2020). https://doi.org:10.1038/s41598-020-63255-6

16 Hardy, J. *et al.* A disorder of cortical GABAergic innervation in Alzheimer's disease. *Neurosci Lett* **73**, 192-196 (1987). https://doi.org:10.1016/0304-3940(87)90016-4

17 Simpson, M. D., Cross, A. J., Slater, P. & Deakin, J. F. Loss of cortical GABA uptake sites in Alzheimer's disease. *J Neural Transm* **71**, 219-226 (1988). https://doi.org:10.1007/bf01245715

18 Bell, K. F. *et al.* The amyloid pathology progresses in a neurotransmitter-specific manner. *Neurobiol Aging* **27**, 1644-1657 (2006). https://doi.org:10.1016/j.neurobiolaging.2005.09.034

19 Garcia-Marin, V. *et al.* Diminished perisomatic GABAergic terminals on cortical neurons adjacent to amyloid plaques. *Front Neuroanat* **3**, 28 (2009). https://doi.org:10.3389/neuro.05.028.2009

20 Lleó, A. *et al.* Changes in Synaptic Proteins Precede Neurodegeneration Markers in Preclinical Alzheimer's Disease Cerebrospinal Fluid. *Mol Cell Proteomics* **18**, 546-560 (2019). https://doi.org:10.1074/mcp.RA118.001290

21 Barthélemy, N. R. *et al.* Highly accurate blood test for Alzheimer's disease is similar or superior to clinical cerebrospinal fluid tests. *Nat Med* **30**, 1085-1095 (2024). https://doi.org:10.1038/s41591-024-02869-z

22 Belleville, S. *et al.* The Consortium for the early identification of Alzheimer's disease–Quebec (CIMA-Q). *Alzheimer's & Dementia:* **11**, 787-796 (2019). https://doi.org:https://doi.org/10.1016/j.dadm.2019.07.003

23 Karikari, T. K. *et al.* Blood phosphorylated tau 181 as a biomarker for Alzheimer's disease: a diagnostic performance and prediction modelling study using data from four prospective cohorts. *Lancet Neurol* **19**, 422-433 (2020). https://doi.org:https://doi.org/10.1016/S1474-4422(20)30071-5

24 Shekhar, S. *et al.* Estimation of Tau and Phosphorylated Tau181 in Serum of Alzheimer's Disease and Mild Cognitive Impairment Patients. *PLoS One* **11**, e0159099 (2016). https://doi.org:10.1371/journal.pone.0159099

25 Thijssen, E. H. *et al.* Plasma phosphorylated tau 217 and phosphorylated tau 181 as biomarkers in Alzheimer's disease and frontotemporal lobar degeneration: a retrospective diagnostic performance study. *Lancet Neurol* **20**, 739-752 (2021). https://doi.org:10.1016/s1474-4422(21)00214-3

26 Postuma, R. B. *et al.* Risk and predictors of dementia and parkinsonism in idiopathic REM sleep behaviour disorder: a multicentre study. *Brain* **142**, 744-759 (2019). https://doi.org:10.1093/brain/awz030